Validation Study on Automatic Methods for the Registration of Carotid Multi-Contrast MR Images

Luca Biasiolli[1], J. Alison Noble[2], Matthew D. Robson[1]

[1]OCMR, [2]IBME, University of Oxford, UK

Abstract. Clinical studies on atherosclerosis agree that multi-contrast MRI is the most promising technique for in-vivo characterization of carotid plaques. Multi-contrast image registration is essential for this application, because it corrects misalignments caused by patient motion during MRI acquisition. To date, it has not been determined which automatic method provides the best registration accuracy in carotid MRI. This study tries to answer this question by presenting an automatic coarse-to-fine algorithm that co-registers multi-contrast images of carotid arteries with sub-pixel accuracy, using three similarity metrics: Correlation Ratio (CR), Mutual Information (MI) and Gradient MI (GMI). Automatic and manual registration were validated using a novel MRI procedure, in which the gold standard is represented by in-plane rigid transformations applied by the MRI system to mimic neck movements. Automatic registration produced lower errors than manual operators. GMI performed slightly better than CR and MI, suggesting that anatomical information improves registration accuracy.

1. Introduction

Atherosclerotic plaque ruptures in the carotid arteries are the main cause of ischemic strokes. Vulnerable plaques can be identified by their morphology and composition. Clinical studies agree that characterization and monitoring of carotid plaques can be successfully performed using multi-contrast MRI (T1, T2 and Proton Density weighted images) [1]. Image registration is essential for this application, because it corrects for patient motion, which causes misalignments between contrast images acquired at different times. Since carotid arteries are small (diameter < 10 mm) with respect to the Field of View (FOV = 150×150 mm) of the images, registration should be focused on the carotid Region of Interest (ROI). Recent in-vivo MRI studies on carotid arteries used Mutual Information [2, 3] or Active Edge Maps [4, 5] for automatic rigid registration of multi-contrast images. However, these registration methods were not thoroughly validated or compared with other suitable candidates for this application.

This article presents an automatic coarse-to-fine technique that performs multi-contrast ROI registration of carotid arteries with sub-pixel accuracy. The proposed method has already been used extensively on patients with different types of atherosclerotic plaques. However, in this clinical application, where the gold standard is not available, it is not possible to measure registration accuracy on patient images. In similar clinical scenarios, manual registration is often used as a reference to validate automatic methods, despite its inter- and intra-operator variability and low sensitivity to misalignments [6]. Other possible validation strategies are controlled phantom studies or software simulations, but synthetic data are simplistic and cannot consider all the challenges faced in real clinical applications. A way to provide a gold standard for rigid registration of real images is to use fiducial markers attached to the subject and visible in all contrast images [7]. Unfortunately, this technique is not suitable for carotid imaging, because surface coils are closely attached to the neck. Thus, in order to measure registration accuracy, we devised a novel MRI validation procedure, which can only be used with healthy subjects who can remain very still for long periods. The method mimics rigid neck movements by applying in-plane transformations (computed by the MRI system during acquisition) to the FOV of contrast images, providing the gold standard registration of carotid MR images. Using this validation method, the registration errors of three similarity metrics (CR, MI, GMI) and three experts (clinically qualified vascular specialists) were measured.

2. Registration Overview

The purpose of multi-contrast MRI registration is to correct for intra-subject motion, which causes misalignments between carotid images acquired at different times. The number of contrast images acquired at the same carotid location in a subject depends on the clinical MRI protocol and can vary between two (typically T1 and T2 or PD and T2 weightings) and more than four (T1, T2, PD and intermediate weightings). Multi-contrast images are sampled within the same FOV and resolution (Figure 1). This study presents an iterative algorithm that co-registers template and reference images (with different contrast weightings) by applying rigid transformations to the template. In the registration process, the initial estimate of the transformation is gradually refined and, at each iteration, the current estimate is used to measure the similarity between template and reference image. Powell's multidimensional direction set algorithm with bisection for one-dimensional optimization [8] is used to find the transformation that maximizes the similarity. A coarse-to-fine strategy improves registration accuracy in the region of interest (ROI) of carotid arteries. The registration algorithm is implemented in MATLAB (The MathWorks, Natick, MA).

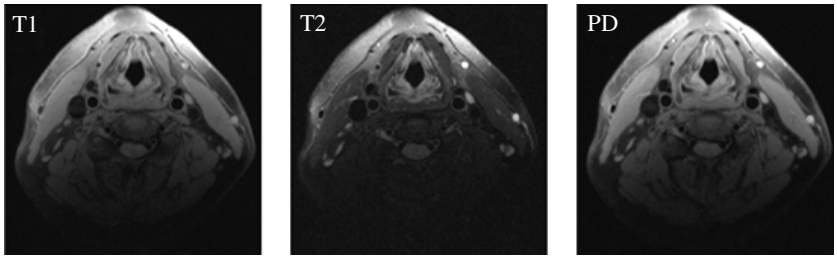

Figure 1. Multi-contrast T1 - T2 - PD - weighted MR images of carotid arteries.

2.1. Image Transformation

Patient motion can be approximated by an in-plane rigid body transformation if two assumptions hold: neck movements through the image plane and tissue deformations in the image plane must both be absent or negligible. The first assumption is valid everywhere, because the degrees of freedom are practically limited to small in-plane rotations and translations by a purpose-built head holder and surface carotid coils. Moreover, MRI slices (~3 mm thick) are less sensitive to through-plane than in-plane (~0.5 mm) movements. The second assumption is valid in the carotid ROI, but not in surrounding regions where breathing and swallowing cause local tissue deformations. Finally, physiological relaxation of tissues during a multi-contrast MRI acquisition (total time is less than 5 minutes) is unperceivable and can be disregarded.

2.2. Similarity Metrics

The degree of alignment between multi-contrast MR images is measured by intensity-based similarity functions. Contrast images are weighted to emphasize one of the tissue magnetic properties (PD, T1 or T2), thus the relationship between signal intensities of the same anatomical feature on different images is not linear. Suitable similarity metrics for this application are Correlation Ratio [9], Mutual Information [10] and Gradient MI [11], because they measure the image information content without requiring any a-priori model of the unknown functional dependence. The information that the template image provides about the reference is assumed to be maximal when the two images are correctly registered.

2.3. Automatic Detection of Carotid Arteries and ROI Registration

The registration of multi-contrast MR images is focused on the carotid ROI to improve the accuracy at plaque location and to avoid areas of tissue deformation. The automatic coarse-to-fine strategy first co-registers the entire images and then only the carotid ROIs with sub-pixel accuracy (Figure 2). Common carotid arteries are automatically detected by the Circular Hough Transform (CHT) of the image gradient [12]. The CHT parameters were initially tested on 8 patients to detect carotid arteries with different plaque types, i.e. imperfect circles with radius from ~1 mm (severe stenosis) to ~7 mm. Peaks in the accumulation matrix of the CHT correspond to approximately circular structures in the image gradient. These can be diseased carotid arteries, but also other vessels or tissues. The following procedure is thus employed to select the carotid arteries using anatomical information.

1. The original MR image is segmented in background (air) and foreground (tissue) using k-means clustering.
2. Only circles with intensity lower than the foreground mean are selected (carotid lumina are hypo-intense).
3. Only the largest connected component of the binary image is selected. Morphological operators with circular structuring elements of different size are applied to close the binary mask.
4. Distance Transform (DT) is applied to the binary mask. The Euclidean distance between each nonzero pixel of the foreground and the nearest zero pixel of the background is calculated. The resulting DT mask represents the shape of the main anatomical structure and the distance of each pixel from the boundaries.
5. The accumulation matrix is weighted by the DT mask. The peaks corresponding to the carotid arteries are enhanced and those closer to the boundaries are reduced.

The automatic carotid detection algorithm proved to be reliable in the presence of different types of atherosclerotic plaques. In a group of 16 patients (different from the test group), 30 carotid arteries were correctly detected and only 2 were misplaced. When automatic detection failed, the user could manually define the carotid ROI.

3. Validation Methodology

The MRI registration validation consisted in simulating rigid body movements of human subjects by applying exact in-plane translations and rotations to the FOV when collecting the images. These transformations were computed by the 1.5T MR system (Sonata, Siemens Medical Solutions, Erlangen, Germany) and defined the gold standard. Registration accuracy of automatic and manual methods was measured by reference to the inverse of the scanner transformation, focusing on the carotid ROI.

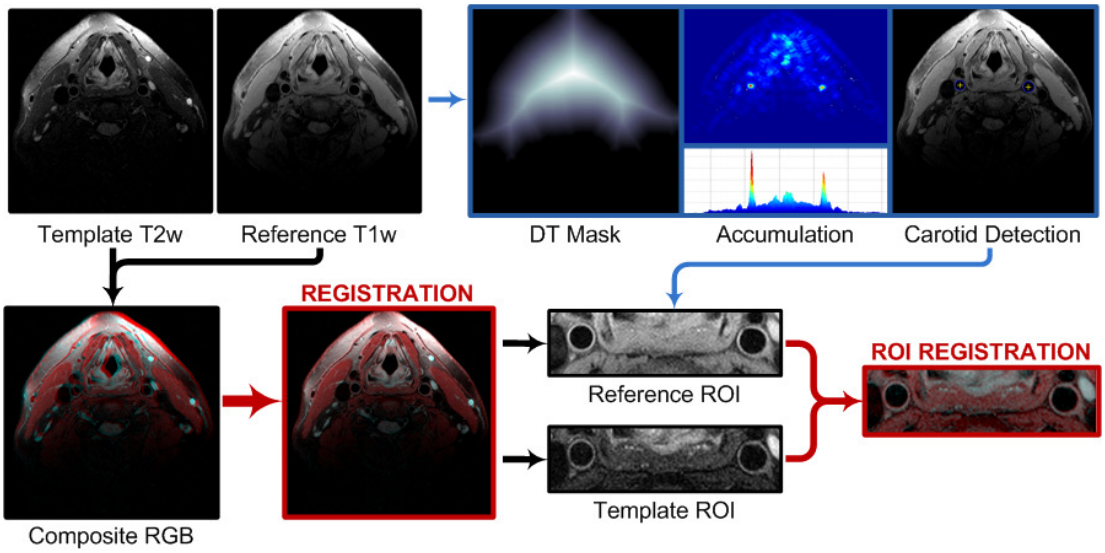

Figure 2. Coarse-to-fine registration example: T2 and T1 weighted images of a healthy volunteer.

Five volunteers and one phantom were imaged following a clinical vascular protocol based on dark-blood Fast Spin Echo (FSE) pulse sequences: Repetition Time (TR) is triggered by an electrocardiogram; SNR is improved by acquiring the MR signal with purpose-built carotid surface coils; signal from flowing blood is suppressed, so that contrast between carotid lumen and wall is enhanced. The scanner operator manually set the MRI slices to be perpendicular to both carotid arteries and 1 cm below the lowest carotid bifurcation. The T1 (TR = 800~1500 ms, Echo Time TE = 12 ms), T2 (TR = 1700~3200 ms, TE = 81 ms) and PD (TR = 1700~3200 ms, TE = 12 ms) weighted images were acquired sequentially at the same slice location, for a total acquisition time shorter than five minutes. MRI slice thickness was 3 mm and in-plane pixel size 468 µm for all the contrast images. The 320×320 k-space, acquired from a FOV of 150 mm, was zero-padded, so that its Fourier Transform produced an interpolated 640×640 image with pixel size of 234 µm.

3.1. Gold Standard

The gold standard transformation exactly aligned multi-contrast MR images of the phantom. In the case of volunteers, head movements were assumed to be much smaller than the scanner transformation and were disregarded. Indeed, subjects were young, healthy and experienced MRI volunteers able to avoid swallowing or other movements during image acquisition (tissue deformation is only caused by breathing). The assumption of subject immobility was later verified by visual inspection. The MRI validation procedure consisted of the acquisition of multi-contrast images in their initial orientation (reference) and after random in-plane transformations (same magnitude of observed patient motion) were applied on the MRI scanner (template). The gold standard transformation was defined by rotation and x-y translations of the MRI scanner between reference and template images in the patient-based Reference Coordinate System (RCS). The mapping of template and reference images to the patient-based RCS were calculated from the attributes of their DICOM files [13], using the following transformation:

$$\begin{bmatrix} P_x \\ P_y \\ P_z \\ 1 \end{bmatrix} = \begin{bmatrix} X_x\Delta i & Y_x\Delta j & 0 & S_x \\ X_y\Delta i & Y_y\Delta j & 0 & S_y \\ X_z\Delta i & Y_z\Delta j & 0 & S_z \\ 0 & 0 & 0 & 1 \end{bmatrix} \begin{bmatrix} i \\ j \\ 0 \\ 1 \end{bmatrix}$$

where P_{xyz} are the coordinates of the pixel (i,j) in the patient-based RCS [mm]; S_{xyz} represent the Image Position (Patient) from the origin of RCS [mm]; X_{xyz} are values from the row direction cosine of Image Orientation (Patient); Y_{xyz} are values from the column direction cosine of Image Orientation (Patient); i is the column index in the image frame; Δi is the column pixel size from Pixel Spacing [mm]; j is the row index in the image frame; Δj is the row pixel size from Pixel Spacing [mm].

3.2. Validation Dataset

Template images were registered to reference images applying the gold standard transformation. All the possible combinations of template-reference image pairs with different contrasts were visually inspected to verify the

assumption that subjects were practically immobile. RGB images composed of contrast image pairs were created (Red channel shows the reference image, whereas both Green and Blue channels show the template image) and visually checked at different magnifications, with particular attention to the alignment of the carotid arteries. A representative group of composite RGB images was selected to form the validation dataset: 9 contrast pairs out of all the MR images acquired from volunteers (3 T2-T1, 3 T2-PD and 3 T1-PD weighted images) and other 3 pairs from the phantom data (1 T2-T1, 1 T2-PD and 1 T1-PD weighted images). For each image pair, the ROI of the carotid arteries was successfully detected by the automatic method presented in section 2.3. The validation dataset was chosen as small as possible because manual registration was very time-consuming (about 3-4 minutes per pair).

4. Results

The accuracy of automatic and manual registration was defined as the mean of the Euclidean distances of carotid centres from their gold standard positions, obtained by applying the inverse scanner transformation to the template images. The validation dataset was manually registered by three experts (clinically qualified vascular specialists), blinded to automatic results and gold standard. They used purpose-built registration software to visually align template and reference images by applying in-plane rigid transformations incrementally (with sub-pixel accuracy in the ROI registration). To assess intra-operator and inter-operator variability, the clinicians performed the manual registration three times each, once per week. Mean, Standard Deviation and Coefficient of Variation (CoV = SD/Mean × 100%) of intra- and inter-operator registration errors were calculated (Table 1).

Table 1. Intra-operator and inter-operator registration error variability.

Variability	***1st Op***	***2nd Op***	***3rd Op***	***Inter-Op***
Mean [µm]	402	259	256	305
SD [µm]	159	90	82	112
CoV [%]	40	35	32	37

In all the automatic registration experiments the rigid transformation was initialized as the identity. Phantom images were used as a control dataset (Figure 3) for the validation of automatic methods. Phantom tubes (representing the arteries) were correctly registered by all the similarity metrics, with results extremely close to the gold standard (Table 2). This was consistent with the registration accuracies obtained on the volunteer dataset (Figure 4), where the three similarity metrics showed analogous behaviour. Mean registration errors were smaller than the pixel size and GMI performed slightly better than CR and MI on the volunteer dataset (Table 2).

Table 2. Mean ± SD of registration errors for volunteer and phantom dataset.

Errors [µm]	**CR**	**MI**	**GMI**	**Manual**
Volunteers	198 ± 92	199 ± 90	181 ± 104	365 ± 102
Phantom	31 ± 14	42 ± 17	23 ± 0	126 ± 35

The difference between automatic and manual methods was significant (GMI-Manual $p = 0.0012$). Figure 3 and Figure 4 compare automatic and manual registration accuracy for every image pair of the validation dataset. All the similarity metrics obtained lower registration errors than manual operators on both phantom and volunteer dataset.

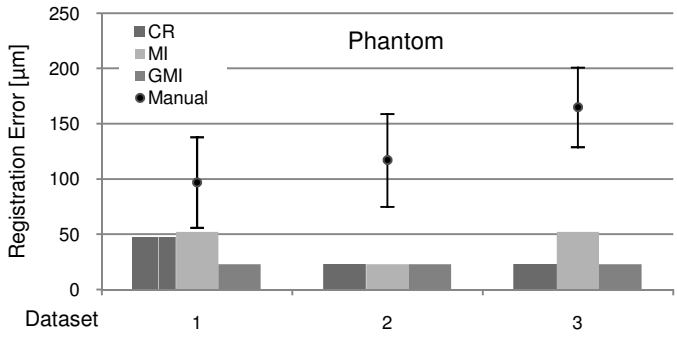

Figure 3. Automatic and manual registration accuracy on phantom dataset.

5. Conclusions

The proposed coarse-to-fine method for multi-contrast image registration is completely automatic and focused on the ROI of carotid arteries. A novel MRI validation method for rigid registration was used to measure the accuracies of three similarity metrics and three manual operators. Correlation Ratio and Mutual Information produced comparable registration errors smaller than the pixel size. GMI performed slightly better, suggesting that spatial information about anatomical features improves registration accuracy. Overall, the automatic method co-registered the carotid arteries more accurately than manual operators on the volunteer dataset. The application of the presented registration strategy is only limited by the assumptions explained in section 2.1. Extreme through-plane movements of patient's neck or large tissue deformation in the carotid ROI are not included in the in-plane rigid transformation model, thus they cannot be corrected. Although the validation study was performed on healthy subjects only, the coarse-to-fine registration method was successfully applied on carotid MR images of atherosclerotic patients. The only known exception to the automatic detection of common carotid arteries is the presence of extremely occlusive plaques.

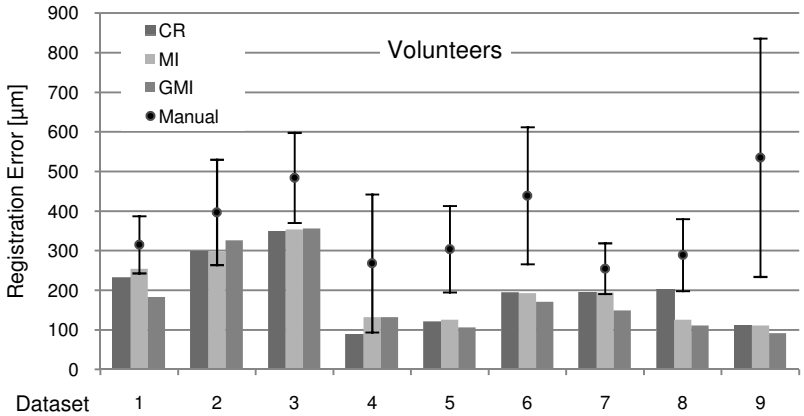

Figure 4. Automatic and manual registration accuracy on volunteer dataset.

References

1. Gillard, J., et al., *Carotid Disease: The Role of Imaging in Diagnosis and Management* 2007, Cambridge, UK: Cambridge University Press.
2. Fei, B., et al., *Three-dimensional automatic volume registration of carotid MR images*, in *Proceedings of the International Conference of IEEE Engineering in Medicine and Biology Society*. 2003. p. 646-648.
3. J.M.A. Hofman, et al., *Quantification of atherosclerotic plaque components using in vivo MRI and supervised classifiers.* Magnetic Resonance in Medicine, 2006. **55**(4): p. 790-799.
4. Kerwin, W. and C. Yuan, *Active edge maps for medical image registration*, in *Medical Imaging 2001: Image Processing, SPIE Vol. 4322*. 2001. p. 516-526.
5. Liu, F., et al., *Automated in vivo segmentation of carotid plaque MRI with Morphology-Enhanced probability maps.* Magnetic Resonance in Medicine, 2006. **55**(3): p. 659-68.
6. Hutton, B.F., et al., *Image registration: an essential tool for nuclear medicine.* European Journal of Nuclear Medicine and Molecular Imaging, 2002. **29**(4): p. 559-577.
7. West, J., et al., *Comparison and Evaluation of Retrospective Intermodality Brain Image Registration Techniques.* Journal of Computer Assisted Tomography, 1997. **21**(4): p. 554.
8. Press, W.H., et al., *Numerical Recipes in C: The Art of Scientific Computing*. 2nd ed. 1992, Cambridge, UK: Cambridge University Press.
9. Roche, A., et al., *The Correlation Ratio as a New Similarity Measure for Multimodal Image Registration*, in *MICCAI'98, Lecture Notes in Computer Science Vol. 1496*. 1998. p. 1115-1124.
10. Viola, P. and W.M. Wells III, *Alignment by Maximization of Mutual Information.* International Journal of Computer Vision, 1997. **24**(2): p. 137-154.
11. Pluim, J.P.W., J. Maintz, and M. Viergever, *Image registration by maximization of combined mutual information and gradient information.* IEEE Trans. on Medical Imaging, 2000. **19**(8): p. 809.
12. Kimme, C., D. Ballard, and J. Sklansky, *Finding circles by an array of accumulators.* Commun. ACM, 1975. **18**(2): p. 120-122.
13. National Electrical Manufacturers Association, *Information Object Definitions*, in *Digital Imaging and Communications in Medicine (DICOM)*. 2007, NEMA: Rosslyn, Virginia.